Experimental Analysis of Linear and Nonlinear Ultrasonic Responses at Fatigue Cracks Using Fundamental Wave Amplitude Difference

疲労き裂における線形・非線形超音波応答の基本波振幅差分による実験的解析

Yoshikazu Ohara[1†], Taisei Umezaki[1], Ewen Carcreff[2], Sylvain Haupert[3], Toshihiro Tsuji[1], and Tsuyoshi Mihara[1] ([1]Tohoku Univ.; [2]The Phased Array Company; [3]Sorbonne Univ.)

小原良和[1†], 梅崎泰生[1], Ewen Carcreff[2], Sylvain Haupert[3], 辻俊宏[1], 三原毅[1] ([1]東北大, [2]The Phased Array Company, [3]ソルボンヌ大)

1. Introduction

Nonlinear ultrasonics has been studied to detect the closed cracks that are undetectable with linear ultrasonics. Recently, various types of nonlinear ultrasonic phased array have been proposed to visualize closed cracks.[1)] One of them is fixed-voltage fundamental wave amplitude difference (FAD).[2-5)] FAD is based on the amplitude dependence of fundamental wave responses to extract all nonlinear components generated at closed cracks. FAD can be readily implemented in commercial PA. We have demonstrated that FAD is useful in high-selectivity imaging of closed cracks.[1-5)] However, the nonlinear scattering behaviors at closed cracks have yet to be fully clarified, which may lead to optimize the measurement conditions.

In this study, we propose to use single focal linear and nonlinear (FAD) images to examine the linear and nonlinear scattering behaviors in detail, in addition to the confocal linear and nonlinear images. We experimentally demonstrate the usefulness of FAD in a closed fatigue crack sample.

2. Single focal and confocal FAD

Figure 1 shows a schematic of single-focus and confocal FAD. Because of the contact vibration of crack faces caused by a large-amplitude incidence, a part of the energy of the fundamental wave is consumed to generate nonlinear components such as higher harmonics and/or subharmonics. Based on this, FAD measures the loss of fundamental wave with increasing the incident wave amplitude. The incident wave amplitude at a transmission focal point (TFP) can be changed with all-elements, odd-elements, and even-elements transmission (T_{All}, T_{Odd}, and T_{Even}) at a fixed excitation voltage. T_{All} is used for a large-amplitude incidence among them, which is also used to create linear image. T_{Odd} and T_{Even} transmission are used for a smaller-amplitude incidence than T_{All}. By taking the subtraction of response for T_{All} from the sum of the responses for T_{Odd} and T_{Even}, all nonlinear components generated at closed cracks can be indirectly measured with canceling the nonlinearity arising from piezoelectric elements and liquid couplant.[1-5)] TFPs are set at multiple angles θ and distances r. For each TFP, the single focal linear and nonlinear images are obtained by following the aforementioned principle. Then, the confocal linear and nonlinear images are created by merging the single-focus images in the vicinity of TFPs, which is typically used. In this study, we use single focal linear and nonlinear image to examine the linear and nonlinear scattering behaviors in detail.

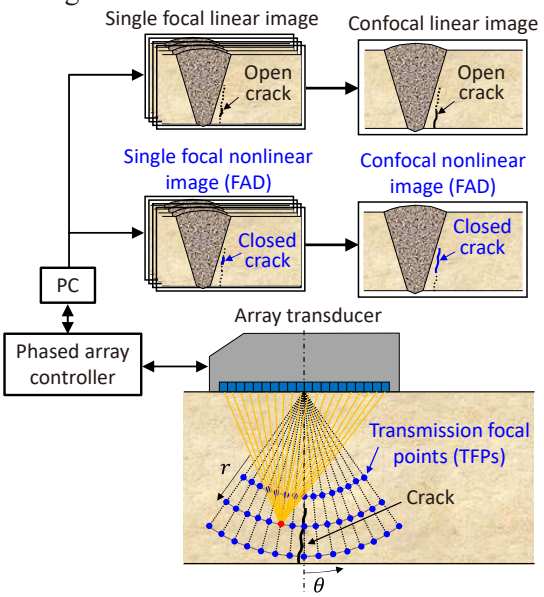

Fig. 1 Schematics of single focal and confocal FAD.

3. Experimental conditions

Figure 2 shows an experimental configuration. We introduced a fatigue crack in an aluminum-alloy A7075 sample by a three-point bending fatigue test. Here the fatigue conditions were the stress intensity factor range ΔK=5 MPa·m$^{1/2}$ and the stress ratio of

R=0.3. A 96-elements array transducer was placed on the top surface and was operated by a phased array controller, OEM-PA 128/128 (AOS, USA). The TFPs were set to $\theta = -5$ to 5° (0.5° step) and r=30 to 34 mm (2 mm step). Each element was excited by a three-cycle burst with 5 MHz and 145 Vp-p. A band-pass filter from 2.5 to 7.5 MHz was employed to extract fundamental components from received waves. We selected the imaging area with 25×25 mm^2 around the cack. The delay-and-sum processing was carried out with 0.5 mm step.

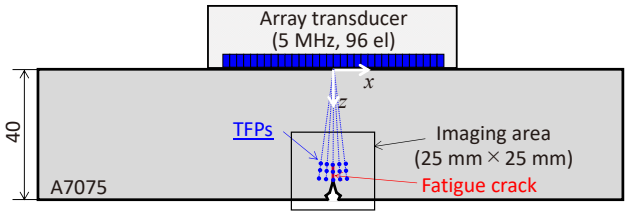

Fig. 2 Experimental conditions.

4. Experimental results

Figure 3 shows the confocal linear and nonlinear images. In the confocal linear image (Fig. 3(a)), the root of the fatigue crack was visualized, whereas the response around the crack tip was weak. On the other hand, in the confocal nonlinear image (Fig. 3(b)), the crack tip was selectively visualized. It shows the usefulness of confocal FAD for closed-crack imaging.

To examine the linear and nonlinear scattering behaviors, **Fig. 4** shows the single focal linear and nonlinear images obtained at the TFPs with $\theta = -2.5°$, 0, and 2.5° at r =30 mm. In the single focal linear images, the root of the fatigue crack was visualized for all θ. In the single focal nonlinear image, the crack tip was observed only for $\theta = 0$. This can be interpreted by assuming that the amplitudes of the focused waves for the TFPs with $\theta = -2.5°$ and 2.5° were smaller at the fatigue crack than a threshold required to cause the nonlinear scattetring. This shows that the nonlinear response is more highly sensitive to the position of TFPs than the linear response. This may imply that setting TFPs with a fine pitch is vital for reliable closed-crack imaging.

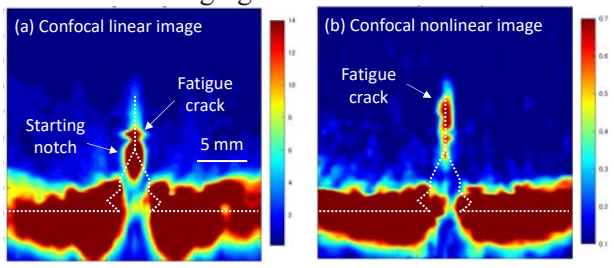

Fig. 3 Confocal linear and nonlinear images of the fatigue crack.

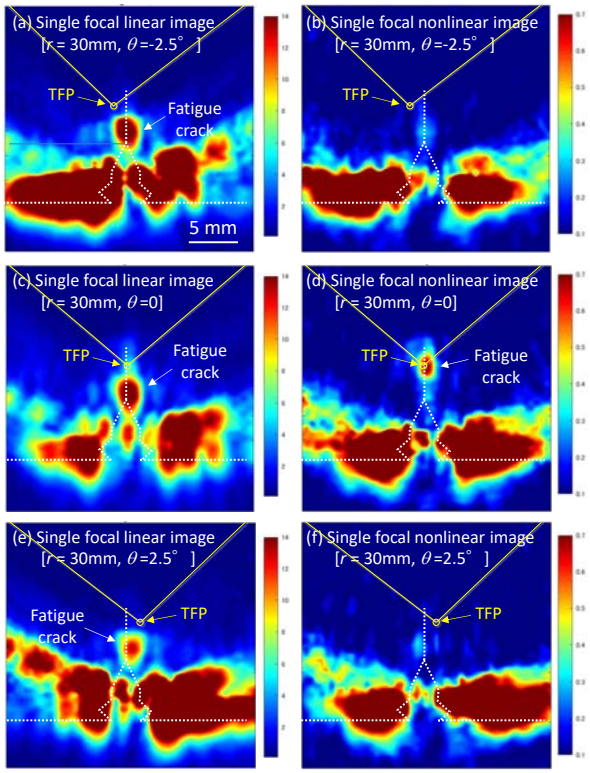

Fig. 4 Single focal linear and nonlinear images for the TFPs with $\theta = -2.5°$, 0, and 2.5° at r =30 mm.

5. Conclusions

We proposed single focal linear and nonlinear (FAD) images to examine the linear and nonlinear scattering behaviors in detail, in addition to confocal linear and nonlinear images. In the confocal nonlinear image, the fatigue crack tip was selectively visualized. In the single focal images, we found that the nonlinear response was more highly sensitive to the position of TFPs than the linear response, which will lead to the optimization of the imaging conditions.

Acknowledgment

This work was partly supported by JSPS KAKENHI (19K21910). The authors thank AOS and dB for the support of the phased array controller (OEM-PA).

References

1) K.-Y. Jhang, C. J. Lissenden, I. Solodov, Y. Ohara and V. Gusev, *Measurement of Nonlinear Ultrasonic Characteristics* (Springer, 2020)
2) S. Haupert, Y. Ohara, E. Carcreff and G. Renaud: Ultrasonics **96** (2019) 132.
3) Y. Ohara, H. Nakajima, S. Haupert, T. Tsuji and T. Mihara: J. Acoust. Soc. Am. **146** (2019) 266.
4) Y. Ohara, H. Nakajima, T. Tsuji and T. Mihara: NDT&E Int. **108** (2019) 102170.
5) Y. Ohara, H. Nakajima, S. Haupert, T. Tsuji and T. Mihara: Jpn. J. Appl. Phys. **59** (2020) SKKB01.